

Long-wavelength radiation by relativistic particles on a circular arc in an external magnetic field

B. M. Bolotovskii and A. V. Serov

P. N. Lebedev Physics Institute, Russian Academy of Sciences, 117924 Moscow, Russia

(Submitted 12 May 1993; revised 5 September 1993)

Zh. Eksp. Teor. Fiz. **105**, 43–49 (January 1994)

We measure experimentally the angular distribution of radiation by relativistic particles in the field of a bending magnet with a rectilinear segment between the point of emergence of the beam and the magnet. We show that the observations are in agreement with the calculated radiation for motion of particles along the actual trajectory. It turns out that the radiation from the rectilinear segment (transition radiation) and from the circular arc (synchrotron radiation) strongly interfere, and therefore dividing the total radiation into transition and synchrotron makes no sense under these experimental conditions.

INTRODUCTION

The radiation from a particle on a prescribed trajectory can be calculated in analytic form. Suppose that the law of motion of the particle is given in the form

$$\mathbf{r}=\mathbf{r}(t). \quad (1)$$

Let us Fourier analyze the vector potential $\mathbf{A}(\mathbf{r},t)$ and the scalar potential $\varphi(\mathbf{r},t)$ with respect to time:

$$\mathbf{A}(\mathbf{r},t)=\int \mathbf{A}_\omega(\mathbf{r})\exp(-i\omega t)d\omega, \quad (2)$$

$$\varphi(\mathbf{r},t)=\int \varphi_\omega(\mathbf{r})\exp(-i\omega t)d\omega.$$

Then the Fourier components $\mathbf{A}_\omega(\mathbf{r})$ and $\varphi_\omega(\mathbf{r})$ are given by¹

$$\mathbf{A}_\omega(\mathbf{r})=\frac{1}{c}\int \frac{\mathbf{j}_\omega(\mathbf{r}')}{|\mathbf{r}-\mathbf{r}'|}\exp\left(\frac{i\omega|\mathbf{r}-\mathbf{r}'|}{c}\right)d\mathbf{r}', \quad (3)$$

$$\varphi_\omega(\mathbf{r})=\int \frac{\rho_\omega(\mathbf{r}')}{|\mathbf{r}-\mathbf{r}'|}\exp\left(\frac{i\omega|\mathbf{r}-\mathbf{r}'|}{c}\right)d\mathbf{r}',$$

where $\mathbf{j}_\omega(\mathbf{r})$ and $\rho_\omega(\mathbf{r})$ are the Fourier components of the current density \mathbf{j} and charge density ρ corresponding to the law of motion (1):

$$\rho=q\delta[\mathbf{r}-\mathbf{r}(t)]=\int \rho_\omega(\mathbf{r})\exp(-i\omega t)d\omega, \quad (4)$$

$$\mathbf{j}=q\mathbf{v}(t)\delta[\mathbf{r}-\mathbf{r}(t)]=\int \mathbf{j}_\omega(\mathbf{r})\exp(-i\omega t)d\omega,$$

where q is the magnitude of the charge and $\mathbf{v}(t)=d\mathbf{r}(t)/dt$ is its velocity.

It follows from Eq. (3) that from every point \mathbf{r}' at which the charge density $\rho_\omega(\mathbf{r}')$ and the current density $\mathbf{j}_\omega(\mathbf{r}')$ are nonzero, a spherical wave

$$\exp(i\omega|\mathbf{r}-\mathbf{r}'|/c)/|\mathbf{r}-\mathbf{r}'| \quad (5)$$

is emitted whose amplitude is proportional to the Fourier component of the current or charge density at \mathbf{r}' , and the total field is determined by superposition of waves of type (5), emitted from every point of the trajectory. It is there-

fore possible in principle to divide the trajectory into several segments and then look for the total field in the form of interference between the fields radiated from individual segments. The subdivision of the trajectory is dictated by convenience. The radiation from certain simple trajectories is well known. Among such simple problems, are, in particular:

(a) radiation from an instantaneous start.^{1,2} It is assumed that the charge particle is at rest up to the instant $t=t_1$, and at $t=t_1$ its velocity jumps from zero to some value \mathbf{v} and remains unchanged thereafter;

(b) radiation from a particle in uniform circular motion (synchrotron radiation)³⁻⁵

(c) radiation from particle in a periodic trajectory $\mathbf{r}(t+T)=\mathbf{r}(t)+\mathbf{l}$, where T is the time period and \mathbf{l} the space period. This radiation is known as undulatory radiation.

The study of these simple cases is justified by the fact that for each of them an exact quantitative investigation is possible by evaluating the integrals in (3) and obtaining analytic expressions for the fields. With the help of these exact expressions, more complicated cases can be considered. In particular, uniform motion of the charge along a finite segment of the path can be represented as a start at the initial point, uniform motion along the specified segment of the path and instantaneous stop at the end of the segment. Similarly, motion of the charge along a finite segment of a circular arc can be viewed as a start at the initial point of the arc, then uniform motion along the arc and instantaneous stop after traversing the specified arc segment.^{6,7} If the trajectory consists of rectilinear segments connected by circular arcs, then it is obvious that the region of integration can be broken up into three segments: rectilinear motion up to the arc, motion along the arc, and a transition to the rectilinear motion at the end of the arc.

However, the division of the trajectory into individual segments is only justified provided the interference between the radiations emitted from different segments is weak. In those cases when the interference is strong, the physical identification of individual segments of the trajectory makes no sense. In an actual experiment it is rare to observe in a pure form the above indicated forms of radiation. Much more often we have to deal with one or another

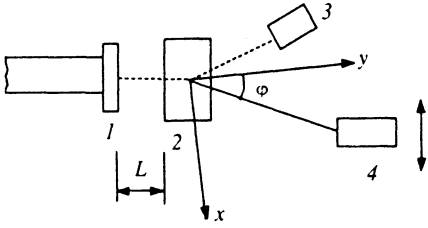


FIG. 1. Experimental layout: 1) flange, 2) turning magnet, 3) Faraday cup, 4) receiver.

combination of start and stop of the accelerated motion. To determine the field, it is then necessary to evaluate the integrals in (3) for the field potentials over the entire physically important region of motion.

If we insert the law of motion (4) into the integral (3), we obtain for the potentials $A_\omega(\mathbf{r})$ and $\varphi_\omega(\mathbf{r})$ the expressions¹

$$A_\omega(\mathbf{r}) = \frac{q}{c} \int_{-\infty}^{\infty} \frac{\mathbf{v}(t)}{|\mathbf{r}-\mathbf{r}(t)|} \exp\left[i\omega\left(t - \frac{|\mathbf{r}-\mathbf{r}(t)|}{c}\right)\right] dt, \quad (6)$$

$$\varphi_\omega(\mathbf{r}) = q \int_{-\infty}^{\infty} \frac{1}{|\mathbf{r}-\mathbf{r}(t)|} \exp\left[i\omega\left(t - \frac{|\mathbf{r}-\mathbf{r}(t)|}{c}\right)\right] dt.$$

If the potentials in the expansions (3) are represented by integrals over space, then the representation (6) contains integration over time. However, it is obvious that if it is possible to divide the integration volume into physically distinct regions in the representation (4), the integrals (6) can be divided accordingly in time. In the case that radiations emitted from individual segments of the trajectory interfere strongly with each other, the division into integration segments turn out to be inconvenient. Below we consider an experiment whose description is not simplified by dividing the trajectory into segments, because the radiations from different segments of the trajectory interfere strongly with one another.

1. EXPERIMENTAL METHOD

The experiment was performed at the Department of High Energy Physics of the P. N. Lebedev Institute of Physics of the Russian Academy of Sciences. The experimental layout is shown in Fig. 1. The source of the relativistic electrons was a microtron. The accelerated current consisted of a sequence of electron bunches each $\cong 10$ mm long, spaced $\cong 100$ mm apart. The energy of the electrons was $E=7.2$ MeV and the current was $I=40$ mA in a $4 \mu\text{s}$ pulse. The particles traversed a beam transporter containing correctors and lenses, and emerged from the microtron vacuum into the atmosphere through a copper foil $100 \mu\text{m}$ thick at the beamline flange 1. The beam passed next through a bending magnet 2 and was absorbed in a Faraday cup 3. The 80-mm wide bending magnet produced a field of amplitude $H=1000$ Oe, in which the particles were deflected by an angle $\alpha \cong 20^\circ$. The part of the orbit from which the electromagnetic radiation was collected was lo-

cated in the air between the foil transversed by the beam and the Faraday cup. That part of the orbit is shown dashed in Fig. 1.

The intensity of the radiation was measured by the receiver 4, containing a D-407 or D-404 silicon point-contact diode and an amplifier. The receiver was located ~ 200 mm from the foil. The front end of the detector was covered by a layer of absorbing rubber, except for the diode window. This prevented possible volume resonances at low frequencies. The D-407 diode has maximum sensitivity at wavelengths of 5–7 mm, and the D-404 diode at 10–12 mm. These wavelengths correspond to the low-frequency end of the spectrum, since the critical wavelength, near the spectral peak, is equal to our case to $\lambda = 4\pi r_0 / 3\gamma^3 = 0.33$ mm, where r_0 is the radius of the orbit and γ is the particle energy in units of mc^2 . The receivers could be remotely moved in the horizontal plane, perpendicular to the beam line. Varying the position of the receiver changed the angle φ between the tangent to the beam orbit at the middle of the bending magnet (the y -axis in Fig. 1) and the direction to the receiver. The angle of observation was varied between $\varphi \cong 0^\circ$ and $\varphi \cong 30^\circ$. In Fig. 1, the angle of observation $\varphi=0$ corresponds to the y -axis, and it can be varied only in one direction (i.e., toward positive values of x) due to the geometry of the setup.

The experimental layout differed from that described in Ref. 7 in that it was possible to change the distance between the flange 1 and the bending magnet 2. In Ref. 7, the electron beam entered the field of the bending magnet immediately upon leaving the foil. The present layout permits moving the bending magnet away from the foil, and therefore the beam trajectory between the foil and the magnetic is rectilinear. It turns out that the character of the angular distribution depends strongly on the distance between the flange and the bending magnet (i.e., the length of the rectilinear segment).

2. DISCUSSION

In the previous experiment,⁷ we studied the angular distribution of the radiation in the absence of the rectilinear segment, when the distance L between the beam injector flange and the face of the bending magnet was equal to zero ($L=0$). In Fig. 2(a) we show the angular distribution of the radiation at $\lambda \cong 12$ mm when that distance equals 25 mm. For comparison, we show the angular distribution for $L=0$ in Fig. 2(b). It is clear that the rectilinear segment leads to interference between radiation emitted from different segments of the trajectory, which produces maxima and minima in the angular distribution. In fact, the magnetic field affects electrons even before they enter the space between the poles, since the magnet has a fringing field. However, first, the fringing field is substantially weaker than the field between the poles, and second, its influence extends out substantially less than the path length over which emission is produced at $\lambda \cong 12$ mm (see below).

It would be natural to attempt to explain the observed radiation as interference of the aforementioned elementary types of radiation. As the electron leaves the foil, it emits

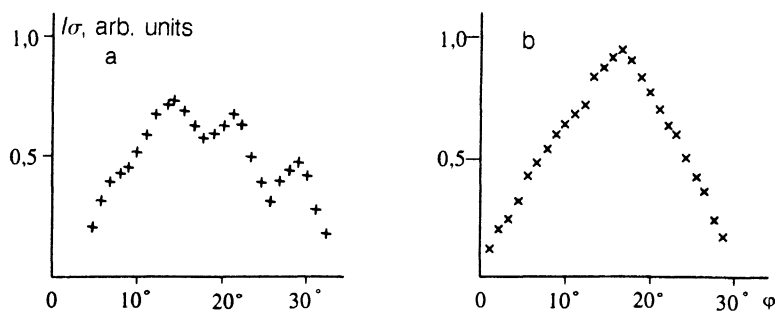


FIG. 2. Experimental horizontal angular distribution of the intensity of the σ -polarized component of the radiation at $\lambda = 12$ mm: a) $L = 25$ mm; b) $L = 0$ mm.

transition radiation (or, what is the same, radiation from an instantaneous start). Upon entering the magnet, the electron starts to move along a circular arc, resulting in synchrotron radiation. It might be thought that the total radiation consists of interference between these two types. However this simple picture fails to describe the observed result. The point is that under the conditions of the experiment the transition radiation has no time to form. Indeed, it can be said that the transition radiation has formed if the rectilinear segment of the trajectory after leaving the foil is long enough for the radiation field to separate in space from the field of the charge. This length (formation path or coherence length) is of order $\lambda\gamma^2$. Under the experimental conditions, $\lambda = 12$ mm and $\gamma = 15$, i.e., the formation path is meters long. On the other hand, the length of the rectilinear segment is 25 mm. Obviously, the transition radiation has no time to form on such a segment. When the length of the rectilinear segment of the trajectory is substantially less than the formation path, the angular distribution of the intensity does not decrease outside the characteristic angle γ^{-1} , but approximates the angular distribution of the classical dipole radiation. Typically, the same can be said about the radiation resulting from the motion of the beam in the field of the bending magnet. Since we are considering long-wavelength radiation ($\lambda \approx 12$ mm), and the length of the arc along which the beams moves in the magnetic field is limited ($\approx 20^\circ$), there is no time for synchrotron radiation to form on this segment.

In view of these considerations it is much more convenient to give up the idea of considering the resultant emission as interference between transition and synchrotron radiation, and from the beginning calculate the total radiation field from Eqs. (3), substituting there the actual trajectory. This trajectory consists of a rectilinear segment 25 mm long, followed by a circular arc of radius $r_0 = 15$ cm and central angle of $\approx 20^\circ$, followed by a rectilinear segment that the electrons follow after passage through the magnet. This last segment is ≈ 60 mm long. The results of the calculations are shown in Fig. 3, where we show I_σ as a function of the angle of observation. We note that the detector has not been calibrated in flux density, and therefore the angular distribution observed experimentally is given in arbitrary units. The calculated ordinates of the angular distribution in Fig. 3 are approximately proportional to the experimental values in Fig. 2(a). Therefore it

can be said that the calculation correctly describes the character of the angular distribution.

Note that in the calculations we took into account the fact that the observation point is at a distance from the region of motion of the charged particles that cannot be considered large in comparison with the size of that region. Were the point of emission sufficiently far away, its radiation could be expressed in terms of the vector potential \mathbf{A}_ω along, as was done in Ref. 7. Under the conditions of the present experiment, the detector is located at a distance from the radiation zone that is comparable to the dimensions of that zone. Therefore both the vector and scalar potential must be known to calculate the field.

It was proposed in Ref. 7 that the intensity modulation observed in the angular distribution were due to high-frequency effects of the radiation. It follows, however, from the present calculations that there is no need for such a proposal. The modulation of the angular distribution is adequately explained by taking into account the actual trajectory. The previously mentioned lack of justification for dividing the trajectory into individual segments applies not only to comparatively low energies and long-wavelength radiation, but also to high energies and optical radiation.

The authors are grateful to Ya. Ruzhichka and V. P. Zrellov for information (see Ref. 8, 9), as well as to V. N. Melekhin for valuable remarks.

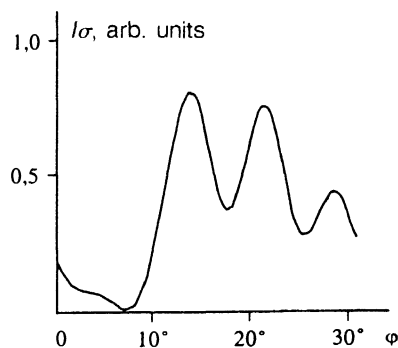


FIG. 3. Angular distribution of the intensity of the σ -polarized component of the radiation, obtained by numerically integrating Eqs. (3): $\lambda = 12$ mm; $L = 25$ mm.

- ¹L. D. Landau and E. M. Lifshitz, *The Classical Theory of Fields*, Pergamon, Oxford (1975).
- ²B. M. Bolotovskii, *Trudy Fiz. Inst. Akad. Nauk* **143**, 95 (1982).
- ³V. L. Ginzburg, *Theoretical Physics and Astrophysics*, Pergamon, Oxford, (1979).
- ⁴A. A. Sokolov and I. M. Ternov, *The Relativistic Electron* [in Russian], Nauka, Moscow (1974).
- ⁵I. M. Ternov and V. V. Mikhailin, *Synchrotron Radiation* [in Russian], Énergoatomizdat, Moscow (1986).
- ⁶V. G. Bagrov, I. M. Ternov, and N. I. Fedosov, *Zh. Eksp. Teor. Fiz.* **82**, 1442 (1982) [Sov. Phys. JETP **55**, 835 (1982)].
- ⁷B. M. Bolotovskii and A. V. Serov, *Zh. Eksp. Teor. Fiz.* **102**, 1506 (1992) [Sov. Phys. JETP **75**, 815 (1992)].
- ⁸Ya. Ruzhichka and V. P. Zrelov, JINR, Preprint No. RI-92-233, Dubna (1992); V. P. Zrelov and Ya. Ruzhichka, JINR Preprint No. RI-92-237, Dubna (1992).
- ⁹V. P. Zrelov, Ya. Ruzhichka, JINR, Preprint No. RI-92-237 (1992).

Translated by Adam M. Bincer